Int J Fract (2010) 162:245–253
DOI 10.1007/s10704-010-9448-y

ORIGINAL PAPER

Modeling dynamic failure in rubber

P. Trapper · K. Y. Volokh

Received: 13 October 2009 / Accepted: 12 January 2010 / Published online: 2 February 2010

Abstract Hyperelasticity with energy limiters is used to model high-velocity penetration in a sheet of natural rubber. Particularly, the Yeoh strain energy function is replaced with a modified expression, which sets a limit for the energy that can be accumulated during deformation. The material constants controlling failure are fitted to the tension tests. The modified strain energy function is plugged in ABAQUS for the three-dimensional explicit analysis of the edge penetration of a stiff elastic projectile into a thin sheet of the natural rubber and the time history of the failure process is tracked.

Keywords Elasticity · Energy limiters · Dynamic · Failure · Rubber · Penetration

1 Introduction

Traditional hyperelastic models of materials impose the so-called growth conditions on the strain energy function, which implies the unlimited increase of the energy with the strain increase. The growth conditions ignore the fact that no material can sustain large enough strains without failure. Evidently, a description of the bulk failure should be a part of the constitutive theories. Such theories were pioneered by Kachanov (1958) and Rabotnov (1963) and they appear by name of Continuum Damage Mechanics (CDM) in the modern literature. Originally, CDM was invented to analyze the gradual failure accumulation and propagation in creep and fatigue. The latter explains why CDM is similar to plasticity theories including (a) the internal damage variable (inelastic strain), (b) the critical threshold condition (yield surface), and (c) the damage evolution equation (flow rule). The subsequent development of the formalism of CDM (Lemaitre and Desmorat 2005) left its physical origin well behind the mathematical and computational techniques and led to the use of CDM for the description of *any* bulk failure (Kachanov 1994). Unfortunately, it is impossible to measure the damage parameter directly and the experimental calibration should be implicit and include both the damage evolution equation and criticality condition.

A physically motivated alternative to the continuum damage mechanics in the cases of failure related with the bond rupture called Virtual Internal Bond (VIB) method was introduced by Gao and Klein (1998) and Klein and Gao (1998). VIB is a multiscale method where different length scales are mixed. Another multiscale model is due to Dal and Kaliske (2009) who included a possible rupture of polymer chains into the constitutive description of rubbers. Of course, a direct appeal to the material structure is very attractive. It should not be missed, however, that the transition from the smaller to larger length scales is always related to an averaging procedure which presumes,

P. Trapper · K. Y. Volokh (✉)
Faculty of Civil and Environmental Engineering,
Technion-Israel Institute of Technology,
32000 Haifa, Israel
e-mail: cvolokh@technion.ac.il

often implicitly, additional assumptions concerning the macroscopic behavior of material that can be revealed in the macroscopic experiments only. Besides, the multiscale link is usually computationally involved what limits its applications to the analysis of bulk failure.

A very simple alternative to CDM and multiscale methods was developed by Volokh (2004, 2007, 2008, 2010)) and Volokh and Trapper (2008), who introduced the energy limiters in the expression of the strain energy. The energy limiters enforce the limit point on the stress-strain curve separating intact and failure behaviors of the bulk analogously to the bond energy of atomic interactions. The developed approach was used in various problems concerning prediction of the failure initiation in materials and structures. In the present work the approach of energy limiters is used for modeling dynamic failure propagation. Particularly, the Yeoh strain energy function is replaced with a modified expression, which sets a limit for the energy that can be accumulated during deformation. The material constants controlling failure are fitted to uniaxial and biaxial tension tests. The modified strain energy function is plugged in ABAQUS for the three-dimensional explicit analysis of the edge penetration of a stiff elastoplastic projectile into a thin sheet of the natural rubber and the time history of the failure process is tracked.

The paper is organized as follows. A short review of the elasticity with energy limiters is given in Sect. 2. The modified Yeoh model for modeling failure of the natural rubber is described in Sect. 3. The finite element simulations of the projectile penetration into a thin rubber sheet are presented in Sect. 4. A brief discussion of the obtained results appears in Sect. 5.

2 Elasticity with energy limiters

To motivate the introduction of energy limiters we briefly describe the continuum-atomistic link. A more detailed exposition of the issue can be found in Volokh (2008), for example.

Interaction of two particles (atoms, molecules, etc) can be described as follows

$$\psi(F) = \varphi(F) - \varphi_0, \quad \varphi_0 = \min_L \varphi(F = 1). \tag{1}$$

Here ψ is the particle interaction potential; F is the one-dimensional deformation gradient which maps the distance between particles from the reference, L, to the current, l, state: $l = FL$. To be specific we choose the Lennard-Jones potential, for example, $\varphi = 4\varepsilon[(\sigma/l)^{12} - (\sigma/l)^6]$, where ε and σ are the bond energy and length constants accordingly. By direct computation we can find the energy limiter or the failure energy, Φ. Indeed, increasing deformation we cannot increase the energy unlimitedly

$$\psi(F \to \infty) = -\varphi_0 = \Phi = \text{constant}. \tag{2}$$

Analogously to the case of the pair interaction it is possible to consider particle assemblies. Assuming the applicability of continuum mechanics to the description of such assemblies, i.e. using the Cauchy-Born rule, it is possible to derive the following stored energy function analogously to (1)

$$\psi(\mathbf{C}) = \langle\varphi(\mathbf{C})\rangle - \langle\varphi\rangle_0\,, \ \langle\varphi\rangle_0 = \min_L \langle\varphi(\mathbf{C} = \mathbf{1})\rangle. \tag{3}$$

Here $\mathbf{C} = \mathbf{F}^T\mathbf{F}$ is the right Cauchy-Green deformation tensor where $\mathbf{F} = \partial\mathbf{y}/\partial\mathbf{x}$ is the deformation gradient of a generic material macro-particle of body Ω occupying position $\mathbf{x}$ at the reference state and position $\mathbf{y}(\mathbf{x})$ at the current state of deformation. The average means $\langle\varphi(\mathbf{C})\rangle = V_0^{-1}\int_{V_0^*} 4\varepsilon[(\sigma/L\,\|\mathbf{C}\|)^{12} - (\sigma/L\,\|\mathbf{C}\|)^6]\,D_V dV$ in the case of the Lennard-Jones potential, where the tensorial norm designates stretch in the bond direction; D_V is the volumetric bond density function; and V_0^* is the integration volume defined by the range of influence of φ; and V_0 is the reference representative volume.

It is important to realize that not all bonds between the material particles are of equal importance in (3) but bonds presenting the weakest links control failure.

Analogously to (2), we can find the energy limiter, Φ, increasing the deformation unlimitedly

$$\Phi = \psi(\|\mathbf{C}\| \to \infty) = -\langle\varphi\rangle_0 = \text{constant}. \tag{4}$$

Thus, *the average bond energy sets a limit for the energy accumulation*. This conclusion generally does not depend on the choice of the particle potential and it is valid for any interaction that includes a possible particle separation.

Contrary to the conclusion above traditional hyperelastic models of materials do not include the energy limiter. The stored energy of hyperelastic materials is defined as

$$\psi = W. \tag{5}$$

Here W is used for the strain energy of the *intact* material, which can be characterized by the following 'growth conditions'

$$\|\mathbf{C}\| \to \infty \Rightarrow \psi = W \to \infty, \tag{6}$$

where $\|\ldots\|$ is a tensorial norm.[1]

In other words, the increasing strain increases the accumulated energy unlimitedly. Evidently, the consideration of only intact materials is restrictive and unphysical. The energy increase of a real material should be limited as it was shown above,

$$\|\mathbf{C}\| \to \infty \Rightarrow \psi \to \Phi = \text{constant}, \tag{7}$$

where the average bond energy, Φ = constant, can be called the *material failure energy*.

Equation (7) presents the fundamental idea of introducing a limiter for the strain energy in the elasticity theory. Such a limiter induces material softening, indicating material failure, automatically. The choice of the limited stored energy expression should generally be material/problem-specific. Nonetheless, a general (or "try first") formula (Volokh 2007) can be introduced to enrich the already existing models of intact materials with the failure description

$$\psi(W) = \Phi\{1 - \exp(-W/\Phi)\}. \tag{8}$$

Where $\psi(W = 0) = 0$ and $\psi(W = \infty) = \Phi$.

Formula (8) obeys condition $\|\mathbf{C}\| \to \infty \Rightarrow \psi(W(\mathbf{C})) \to \Phi$ and, in the case of the intact material behavior, $W << \Phi$, we have $\psi(W) \approx W$ preserving the features of the intact material.

3 Yeoh model of natural rubber enhanced with a failure description

It is evident from examples reviewed in Volokh (2008) that formula (8) is useful for a description of smooth failure with a flat limit point on the stress-strain curve which corresponds to a gradual process of the bond rupture. The gradual rupture is typical of some soft biological tissues. In the case of more abrupt bond ruptures typical of rubbers, however, a much sharper transition to the material instability occurs. To describe sharp transitions to failure the following universal formula for the strain energy density was proposed by Volokh (2010)

$$\psi = \frac{\Phi}{m}\left\{\Gamma\left(\frac{1}{m},\ 0\right) - \Gamma\left(\frac{1}{m},\ \frac{W^m}{\Phi^m}\right)\right\}, \tag{9}$$

where the upper incomplete gamma function is used $\Gamma(s,\ x) = \int_x^\infty t^{s-1}\exp(-t)dt$.

[1] We do not specify the tensorial norm intentionally because various norms can be used.

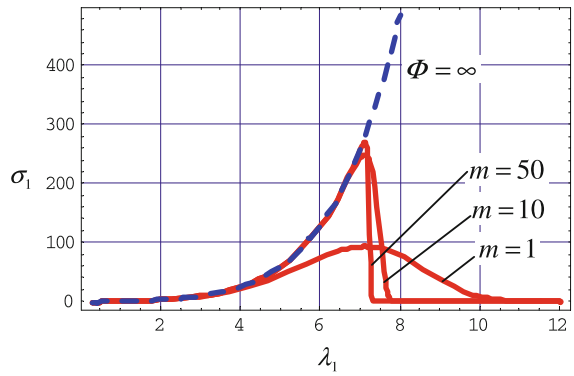

Fig. 1 Cauchy stress (MPa) versus stretch in uniaxial tension. *Blue dashed line* designates intact Yeoh model. *Red lines* designate Yeoh model with energy limiters for varying m

Differentiating the modified strain energy with respect to the right Cauchy-Green tensor we get the following constitutive equation for the Cauchy stress

$$\begin{aligned}\boldsymbol{\sigma} &= 2(\det\mathbf{F})^{-1}\mathbf{F}\frac{\partial\psi}{\partial\mathbf{C}}\mathbf{F}^T \\ &= 2(\det\mathbf{F})^{-1}\mathbf{F}\frac{\partial W}{\partial\mathbf{C}}\mathbf{F}^T\exp(-\frac{W^m}{\Phi^m}).\end{aligned} \tag{10}$$

The new material parameter m controls the sharpness of the transition to material instability on the stress strain curve. Increasing m it is possible to simulate the catastrophic rupture of the internal bonds. In the case of $m = 1$ we reproduce (8). We should mention that the limiting value of the failure energy is $\Phi\,\Gamma(1/m,\ 0)/m$ and it reduces to Φ for $m = 1$.

We apply (10) to the Yeoh (1990) model of natural rubber calibrated by Hamdi et al. (2006)

$$\begin{aligned}W = C_{10}(I_1 - 3) + C_{20}(I_1 - 3)^2 + C_{30}(I_1 - 3)^3,\\ \det\mathbf{F} = 1,\end{aligned} \tag{11}$$

where $I_1 = \text{tr}\mathbf{C}$ and $C_{10} = 0.298\,\text{MPa}$, $C_{20} = 0.014\,\text{MPa}$, $C_{30} = 0.00016\,\text{MPa}$.

In order to fit the constants controlling failure, Φ and m, the critical failure stretch $\lambda_{cr} = 7.12$ found by Hamdi et al. (2006) in uniaxial tension tests was used. Based on this data Volokh (2010) introduced the following modified Yeoh models (Fig. 1) with varying parameter $m = 1, 10, 50$

$$\psi_m = \frac{\Phi_m}{m}\left\{\Gamma\left(\frac{1}{m},\ 0\right) - \Gamma\left(\frac{1}{m},\ \frac{W^m}{\Phi_m^m}\right)\right\}, \tag{12}$$

where $\Phi_{NR1} = 58.6\,\text{MPa}$, $\Phi_{NR10} = 79.9\,\text{MPa}$, and $\Phi_{NR50} = 69.27\,\text{MPa}$.

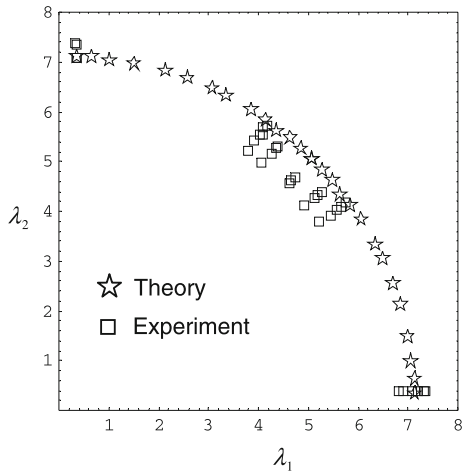

Fig. 2 Critical failure stretches in biaxial tension

It is remarkable that models with large parameter m depart from the stress-strain curve of the intact material much later than models with small m. Moreover, the models with large m correspond to steep failure of material bonds which is reasonable for rubber.

It is interesting to compare the critical failure stretches predicted by (12) with the experimental results reported by Hamdi et al. (2006) in biaxial tension tests—Fig. 2.

The comparison is very encouraging, especially, taking into account that the biaxial data was not used for the calibration of the theory.

4 Finite element simulations

We implement the described analytical model with the help of the user-defined subroutine VUMAT within ABAQUS (2008) finite element software. To account for the incompressibility of the natural rubber we slightly modify the theoretical model penalizing volumetric changes as follows

$$\hat{\psi}_m = \psi_m + \alpha(I_3 - 1) - \beta \ln I_3, \tag{13}$$

where $I_3 = \det \mathbf{C}$, and α and β are material constants.

The relationship between the material constants is established by using condition of zero residual stresses

$$\boldsymbol{\sigma}(\mathbf{F} = \mathbf{1}) = \mathbf{0}. \tag{14}$$

For the considered model we have

$$\boldsymbol{\sigma} = \frac{2}{\sqrt{I_3}} \left\{ I_3 \frac{\partial \hat{\psi}_m}{\partial I_3} \mathbf{1} + \frac{\partial \hat{\psi}_m}{\partial I_1} \mathbf{B} \right\}, \tag{15}$$

where $\mathbf{B} = \mathbf{F}\mathbf{F}^T$ is the left Cauchy-Green deformation tensor, or

$$\boldsymbol{\sigma} = 2\sqrt{I_3} \left(\alpha - \frac{\beta}{I_3} \right) \mathbf{1} + \frac{2}{\sqrt{I_3}} (C_{10} + 2C_{20}\,(I_1 - 3) + 3C_{30} \left(I_1 - 3 \right)^2 \Big) \mathbf{B} \exp\left(-\frac{W^m}{\Phi_m^m} \right). \tag{16}$$

Substituting (16) in (14) we get

$$\boldsymbol{\sigma} = 2(\alpha - \beta + C_{10})\mathbf{1} = \mathbf{0}, \tag{17}$$

and, consequently,

$$\beta = \alpha + C_{10}. \tag{18}$$

Thus defining $\alpha \approx \beta >> C_{10}$ we enforce incompressibility in computations. Of course, there is a variety of alternative ways to account for the approximate incompressibility of the material.

Finally, we define the criteria for the element erosion and deletion as follows

$$\psi_m - \frac{\Phi_m}{m} \Gamma(\frac{1}{m},\ 0) \leq \text{Tolerance} = 10^{-2}. \tag{19}$$

Deleting the failed elements is necessary in order to prevent from the material healing when a returning wave of deformation can restore the failed elements. The element 'killing' or removing procedure is an integral part of the commercial finite element software dealing with the failure simulations. Usually, the elements are removed forcefully when a criterion of the removal is obeyed. In our case, however, contrary to the widespread finite element technologies there is no need to kill the elements—they die on their own—and it is only necessary remove the failed elements.

First, we simulate 3D impact and penetration of a projectile on the edge of a plate fixed at its bottom and top—Fig. 3.

The projectile is elastic with mass density, $\rho = 7.85\,\text{g/cm}^3$; elasticity modulus, $E = 207,000\,\text{MPa}$; Poisson ratio, $\nu = 0.3$; and its circle edge as shown in Fig. 4.

Since the plate is thin, the failed material is not stored and there is no need to consider its hydrostatic resistance. The rubber sheet has mass density $\rho = 0.98\,\text{g/cm}^3$ and the elastic constants: $C_{10} = 50 \cdot 0.298\,\text{MPa}$, $C_{20} = 50 \cdot 0.014\,\text{MPa}$, $C_{30} = 50 \cdot 0.00016\,\text{MPa}$, $\alpha = \beta = 5,000\ \text{MPa}$, $\Phi_{NR10} = 79.9\,\text{MPa}$, $m = 10$. We scaled the stiffness coefficients derived from the statical tests by factor of 50 in order to mimic some dynamic stiffening.[2]

[2] Unfortunately, we are unaware of the experimental data on the dynamic stiffening of rubber and we use the scaling factor voluntarily.

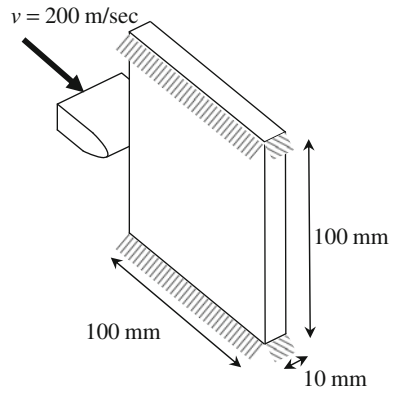

Fig. 3 Low-velocity penetration of a projectile into a rubber plate

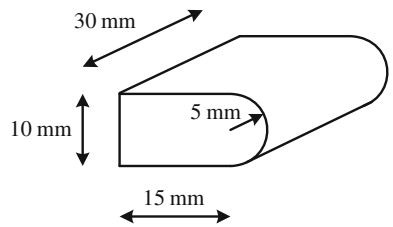

Fig. 4 Elastic projectile

Two series of impact simulations with meshes of $43,200 = 60 \times 60 \times 12$ and $102,400 = 80 \times 80 \times 16$ eight-node brick elements at the velocity of 200 m/s are shown in Fig. 5.

The failure develops as follows. The projectile penetrates the plate destroying rubber elements ahead of it. The dipper is the penetration the more elements of the plate are destroyed. The time evolution of the volume of the eroded elements is presented in Fig. 5a and c and it reflects two stages of failure. At the first stage—up to 0.8 ms—the projectile cuts the plate. At the second stage—up to 1.8–1.9 ms—the failure proceeds for some time without the impact of the projectile because of the interaction of the reflected deformation waves. After 1.8–1.9 ms the graph becomes horizontal, i.e. there is no further element erosion. Figure 5b shows that the projectile propagates by destroying a rubber layer of the thickness of two finite elements. In other words, the projectile propagates a crack ahead of it. The reasons for such behavior, in our opinion, are the following: (1) the material is soft and it can undergo large deformations; (2) the projectile is relatively sharp; (3) the velocity of the penetration is relatively low. Essentially, the observed failure propagation is analogous to cutting a rubber sheet with the help of scissors which also creates a crack that does not propagate on its own and requires a constant 'support' from the scissors. An important observation is that failure tends to localize in a thin band and, consequently the calculations exhibit the 'pathological' mesh-sensitivity. Indeed, the smaller are the elements the thinner is the band. The latter is reflected in Fig. 5c where the energy dissipation is smaller for the finer mesh.

Next, we simulate 3D impact and penetration of another projectile—Fig. 6.

All material parameters remain the same as in the previous simulation. The main differences with the previous simulation are the high velocity of the projectile and its flat contact surface. Three series of impact simulations with meshes of $30,240 = 60 \times 42 \times 12$, $48,020 = 70 \times 49 \times 14$, and $71,680 = 80 \times 56 \times 16$ eight-node brick elements at the velocity of 1500 m/s are shown in Fig. 7.

Similar to the previous simulation, the evolution of the volume of the eroded elements reflects two stages of failure. At the first stage—up to 0.05 ms—the projectile cuts the plate. At the second stage—up to 0.1–0.15 ms—the failure proceeds for some time because of the interaction of the reflected deformation waves. After 0.1–0.15 ms the graph becomes horizontal, i.e. there is no further element erosion. Contrary to the previous simulation, however, Fig. 7b shows that the projectile propagates by massively destroying finite elements ahead of the cutting edge. There is no evidence of the failure localization into thin bands. Since failure does not localize there is no expectation of the 'pathological' mesh-sensitivity. Indeed, up to time 0.05 ms the energy dissipation is practically not affected by the size of the mesh. Some difference between the different meshes appears in the energy dissipation after the cutting is accomplished. The latter can probably be a result of the excessive distortion of finite elements though the ABAQUS indicator of the element distortion did not alarm in these simulations. The fact that in the absence of the failure localization the results converge with the mesh refinement has also been observed in the simulation of the impact and penetration in brittle materials by Trapper and Volokh (2010).

Remark 4.1 The presented algorithm does not preserve mass. Evidently, the weight of two cut pieces of the plate after penetration is smaller than the weight of the intact plate before penetration. It seems reasonable that

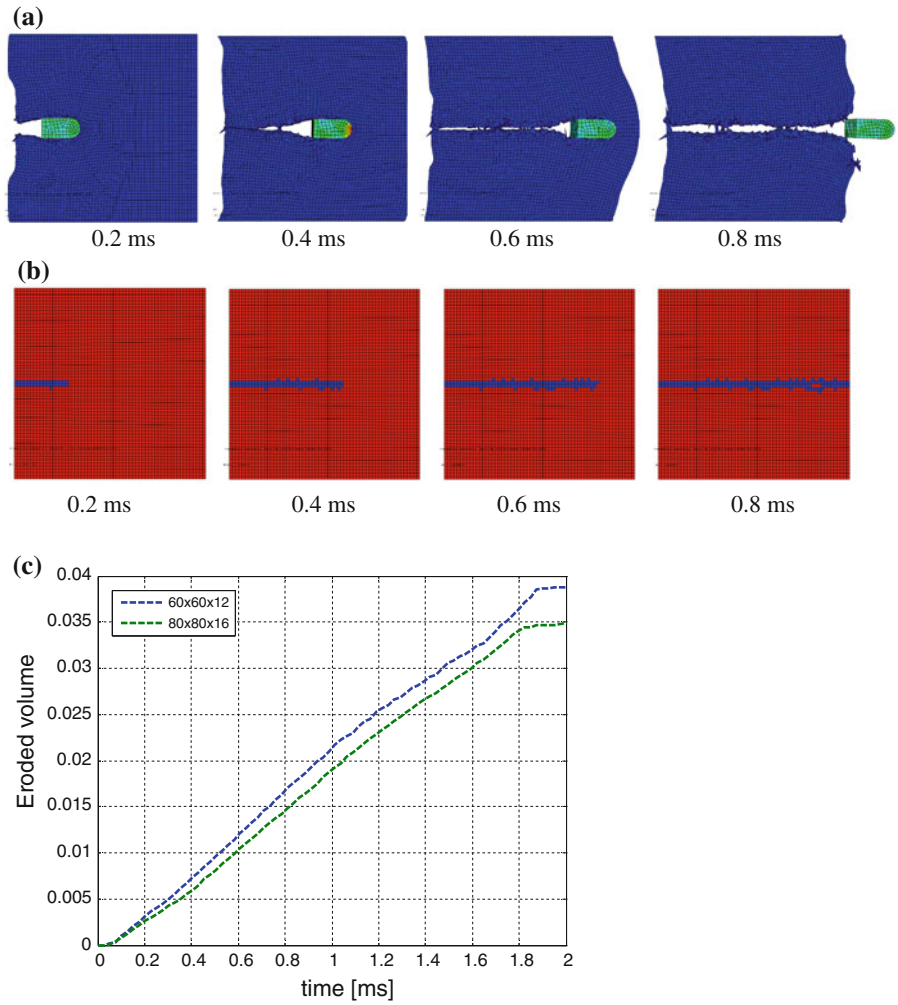

Fig. 5 Projectile penetration at the speed of 200 m/s: **a** projectile propagation at 0.2, 0.4, 0.6, and 0.8 ms, **b** eroded elements at 0.2, 0.4, 0.6, and 0.8 ms, **c** relative eroded volume (dissipated energy) for various finite element meshes

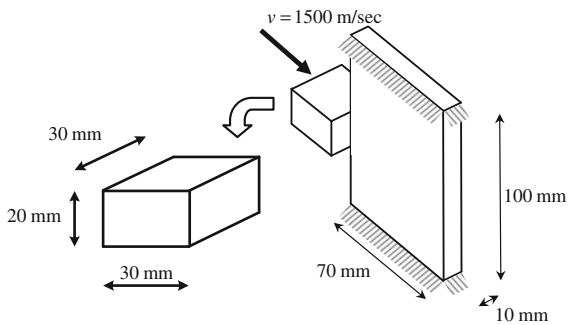

Fig. 6 High-velocity penetration of a projectile into a rubber plate

mass is not preserved in the considered example where the crashed material is free to leave the plate. However, the algorithm must be modified when the projectile penetrates a massive body where crashed material is stored: the overall mass of the intact and crashed material should be conserved. The later situation takes place when soil is penetrated.

5 Concluding remarks

Hyperelastic models of rubberlike solids allow accumulating strain energy unlimitedly. The latter is unphysical and the possibility of material failure should be included in the theoretical description. A way to describe failure is to introduce energy limiters in the expression of the strain energy. This idea is essentially an extension of the description of two-particle separation to large amounts of particles—continuum. The methods of elasticity with energy limiters are dramatically simpler than the existing methods of CDM, for

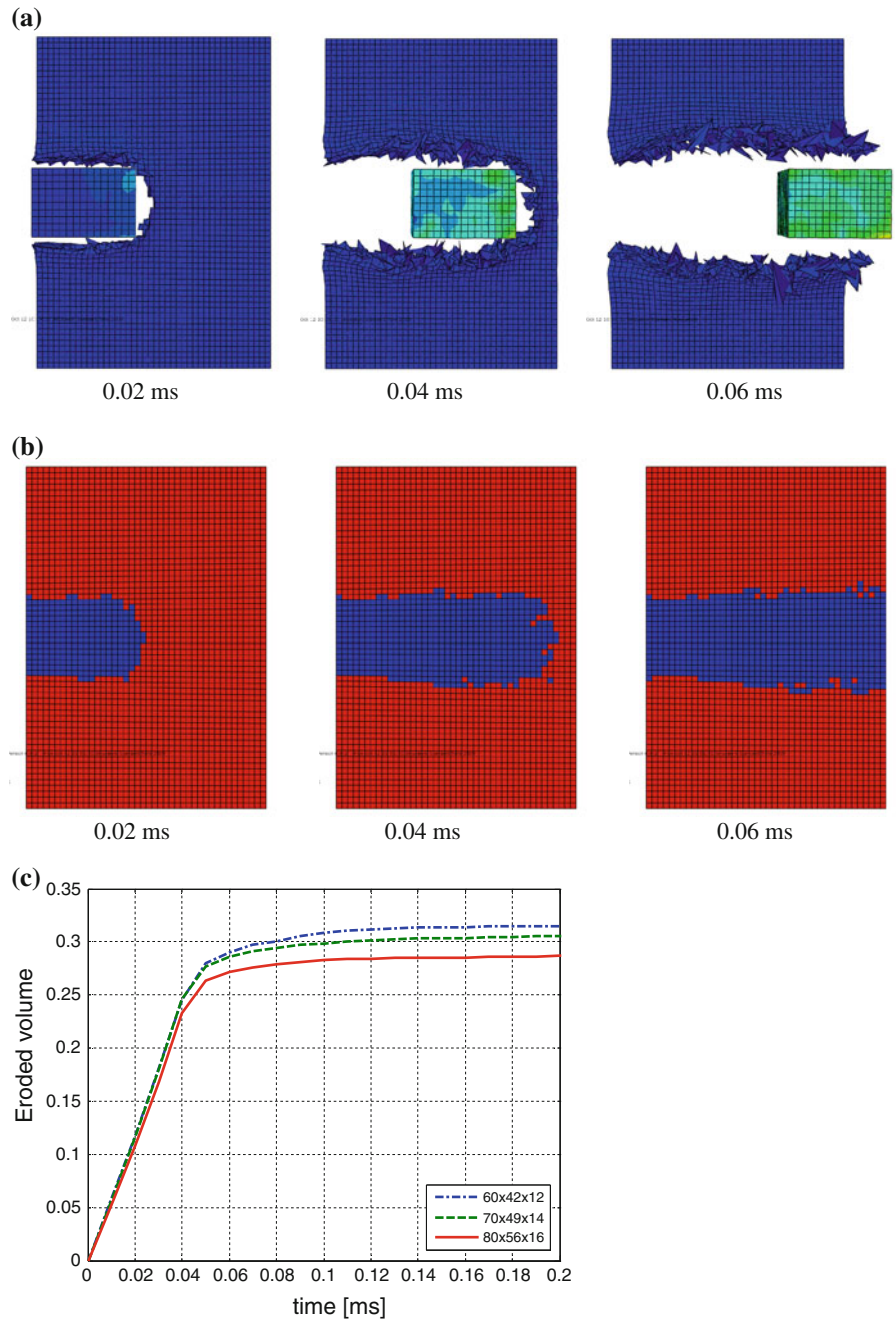

Fig. 7 Projectile penetration at the speed of 1,500 m/s: **a** projectile propagation at 0.02, 0.04, and 0.06 ms, **b** eroded elements at 0.02, 0.04, and 0.06 ms, **c** relative eroded volume (dissipated energy) for various finite element meshes

example, that are traditionally used for modeling bulk failure—Table 1.

It should not be missed, however, that the elasticity with energy limiters is not a universal substitute for CDM. Materials exhibiting essential inelastic deformations are beyond the scope of the methods of energy limiters.

We used the Yeoh hyperelastic model enhanced with the energy limiters to simulate the low- and high-velocity penetration of a stiff elastic projectile into a thin plate made out of natural rubber. This is probably the first reported 3D simulation of the dynamic failure of rubber during the high-velocity penetration though simulations of the dynamic fracture of rubber can be

Table 1 Comparison of continuum damage mechanics and the methods of energy limiters

	Damage internal variables	Damage threshold condition	Damage evolution equation
Damage mechanics	Yes	Yes	Yes
Energy limiters	No	No	No

found in Marder (2006). We observed that in the case of the relatively slow penetration of a relatively sharp projectile the material failure localizes in a thin band—crack-like failure. This failure mode exhibits 'pathological' mesh-sensitivity and requires regularization. It is also interesting that there is a quite long period after the full cut of the plate when the failure process proceeds due to the reflecting deformation waves—the post-cut failure. We also observed that in the case of the high-velocity penetration of a flat projectile the material failure is massive and it does not tend to localize in thin cracks. This type of failure is described reasonably well by the proposed model. It does not exhibit the 'pathological' mesh-sensitivity and it does not require the special regularization procedures. We also observed that in the case of the high-velocity impact the post-cut failure was small.

Of course, even in the absence of sharp localizations or in the cases where such localizations are directly enforced in analysis high strain gradients and the bifurcation multiplicity are two main sources of mesh-sensitivity. The necessity to treat high strain gradients by refining the mesh is not specific of the material models with softening—this is the central issue of the finite element analysis as a whole. The bifurcation multiplicity is more typical of the models with softening. It is worth noting that both bulk and surface (cohesive zone) models can suffer from the bifurcation multiplicity. The latter may trigger some uncertainty, i.e. mesh dependency, of numerical simulations. It seems reasonable to assume that the numerical uncertainty reflects the real physical uncertainty of the problem of material failure. Unfortunately, one can regularize mathematics not physics.

Finally, we should make some remarks on the failure modes. People often mean cracks when they think about failure. That is not always true because there are two possible modes of failure: volumetric failure or massive crash and surface failure or crack. The same solid can exhibit different failure modes under different loads. Consider, for example a piece of ice hitting a glass window. If the ice is hand-thrown then typically the window splits into pieces separated by running cracks. If the ice is shot at high speed then it can drill an accurate hole in the glass without propagating cracks and destroying the entire window. The simulations presented in our work also give an illustration of two failure modes. The question is whether the different failure modes can be described by the same analytical and computational methods or whether the different methods (Song et al. 2008) can describe the same failure modes. The positive answer is desirable yet not evident. The problem is that the methods based on the description of surface failure tend to prescribe the crack mode in advance while the methods based on the description of bulk crash cannot handle sharp localizations of failure. Moreover, the situation is worsening by the fact that we are not necessarily able to predict the physical mode of failure in advance in order to choose a suitable theoretical and computational description.

Acknowledgments This research was supported by the Israeli Ministry of Construction and Housing.

References

ABAQUS (2008) Version 6.8, H.K.S Inc., Pawtucket, RI

Dal H, Kaliske M (2009) A micro-continuum-mechanical material model for failure of rubber- like materials: Application to ageing-induced fracturing. J Mech Phys Solids 57: 1340–1356

Gao H, Klein P (1998) Numerical simulation of crack growth in an isotropic solid with randomized internal cohesive bonds. J Mech Phys Solids 46:187–218

Hamdi A, Nait Abdelaziz M, Ait Hocine N, Heuillet P, Benseddiq N (2006) A fracture criterion of rubber-like materials under plane stress conditions. Polymer Test 25:994–1005

Kachanov LM (1958) Time of the rupture process under creep conditions. Izvestiya Akademii Nauk SSSR, Otdelenie Teckhnicheskikh Nauk 8, pp 26–31 (in Russian)

Kachanov M (1994) On the concept of damage in creep and in the brittle-elastic range. Int J Damage Mech 3:329–337

Klein P, Gao H (1998) Crack nucleation and growth as strain localization in a virtual-bond continuum. Engng Fract Mech 61:21–48

Lemaitre J, Desmorat R (2005) Engineering damage mechanics: ductile, creep, fatigue and brittle failures. Springer, Berlin

Marder M (2006) Supersonic rupture of rubber. J Mech Phys Solids 54:491–532

Rabotnov YN (1963) On the equations of state for creep. In: Progress in applied mechanics (Prager Anniversary Volume), MacMillan, New York

Song JH, Wang H, Belytschko T (2008) A comparative study on finite element methods for dynamic fracture. Comput Mech 42:239–250

Trapper P, Volokh KY (2010) Elasticity with energy limiters for modeling dynamic failure propagation. Submitted (available on http://imechanica.org/node/6707)

Volokh KY (2004) Nonlinear elasticity for modeling fracture of isotropic brittle solids. J Appl Mech 71:141–143

Volokh KY (2007) Hyperelasticity with softening for modeling materials failure. J Mech Phys Solids 55:2237–2264

Volokh KY (2008) Multiscale modeling of material failure: from atomic bonds to elasticity with energy limiters. J Multiscale Comp Engng 6:393–410

Volokh KY (2010) On modeling failure of rubberlike materials. Submitted (available on http://imechanica.org/node/6707)

Volokh KY, Trapper P (2008) Fracture toughness from the standpoint of softening hyperelasticity. J Mech Phys Solids 56:2459–2472

Yeoh OH (1990) Characterization of elastic properties of carbon black filled rubber vulcanizates. Rubber Chem Technol 63:792–805